



# Retinal dysfunction induced in a mouse model of unilateral common carotid artery occlusion

Deokho Lee<sup>1,2,\*</sup>, Heonuk Jeong<sup>1,2,\*</sup>, Yukihiro Miwa<sup>1,2,3</sup>, Ari Shinjima<sup>1,2</sup>, Yusaku Katada<sup>1,2</sup>, Kazuo Tsubota<sup>2,4</sup> and Toshihide Kurihara<sup>1,2</sup>

<sup>1</sup>Laboratory of Photobiology, Keio University School of Medicine, Tokyo, Japan

<sup>2</sup>Department of Ophthalmology, Keio University School of Medicine, Tokyo, Japan

<sup>3</sup>Animal eye-care, Tokyo Animal Eye Clinic, Tokyo, Japan

<sup>4</sup>Tsubota Laboratory, Inc., Tokyo, Japan

\*These authors contributed equally to this work.

## ABSTRACT

**Background.** Retinal ischemic stresses are associated with the pathogenesis of various retinal vascular diseases. To investigate pathological mechanisms of retinal ischemia, reproducible, robust and clinically significant experimental rodent models are highly needed. Previously, we established a stable murine model of chronic hypoperfusion retinal injuries by permanent unilateral common carotid artery occlusion (UCCAO) and demonstrated chronic pathological processes in the ischemic retina after the occlusion; however, retinal functional deficits and other acute retinal ischemic injuries by UCCAO still remain obscure. In this study, we attempted to examine retinal functional changes as well as acute retinal ischemic alterations such as retinal thinning, gliosis and cell death after UCCAO.

**Methods.** Adult mice (male C57BL/6, 6–8 weeks old) were subjected to UCCAO in the right side, and retinal function was primarily measured using electroretinography for 14 days after the surgery. Furthermore, retinal thinning, gliosis and cell death were investigated using optical coherence tomography, immunohistochemistry and TUNEL assay, respectively.

**Results.** Functional deficits in the unilateral right retina started to be seen 7 days after the occlusion. Specifically, the amplitude of b-wave dramatically decreased while that of a-wave was slightly affected. 14 days after the occlusion, the amplitudes of both waves and oscillatory potentials were significantly detected decreased in the unilateral right retina. Even though a change in retinal thickness was not dramatically observed among all the eyes, retinal gliosis and cell death in the unilateral right retina were substantially observed after UCCAO.

**Conclusions.** Along with previous retinal ischemic results in this model, UCCAO can stimulate retinal ischemia leading to functional, morphological and molecular changes in the retina. This model can be useful for the investigation of pathological mechanisms for human ischemic retinopathies and furthermore can be utilized to test new drugs for various ischemic ocular diseases.

Submitted 1 December 2020

Accepted 2 June 2021

Published 21 June 2021

Corresponding authors

Kazuo Tsubota, tsubota@z3.keio.jp

Toshihide Kurihara,

kurihara@z8.keio.jp

Academic editor

Vladimir Uversky

Additional Information and  
Declarations can be found on  
page 15

DOI 10.7717/peerj.11665

© Copyright  
2021 Lee et al.

Distributed under  
Creative Commons CC-BY 4.0

OPEN ACCESS

**Subjects** Biochemistry, Zoology, Ophthalmology

**Keywords** Retina, Hypoxia, Electroretinography, Ischemia, Carotid artery, Ophthalmic artery, Ocular ischemic syndrome, Stroke, Hypoperfusion, Retinal gliosis

## INTRODUCTION

Retinal ischemia is a general cause of visual impairment and blindness all over the world (*Osborne et al., 2004*). It is associated with a huge range of clinical ocular disorders and diseases such as diabetic retinopathy, glaucoma, optic neuropathies and stroke (*Dattilo, Newman & Biousse, 2018; Fouda et al., 2020; Minhas, Morishita & Anand, 2012; Osborne et al., 2004*). As oxygen (directly referred to as “blood”) in the retina is supplied through the ophthalmic artery originated from the internal carotid artery, one of two branches of the common carotid artery (CCA), animal models by common carotid artery occlusion or stenosis (CCAO or CCAS) have been used to understand the pathogenesis of retinal ischemia (*Crespo-Garcia et al., 2018; Davidson et al., 2000; Lavinsky et al., 2006; Lee et al., 2020b; Qin et al., 2019; Sun et al., 2019; Venkat, Chopp & Chen, 2015; Wellons Iii et al., 2000; Yamamoto et al., 2006; Yang et al., 1997*).

In human, CCAO or CCAS is a devastating cause of ocular ischemic syndrome (*Faries et al., 2006*). Ocular ischemia resulting from CCAO or CCAS has gradually received attention in that several ocular disorders, such as ischemic optic neuropathy, diabetic retinopathy and glaucoma, are suggested to be involved with cardiovascular diseases-associated retinal ischemic states (*Chou et al., 2018; Drinkwater, Davis & Davis, 2020; Harris et al., 1999; Osborne et al., 2004*). Therefore, CCAO or CCAS has been attempted to develop animal models for such retinal ischemic diseases. However, several previous studies demonstrated that experimental models (mice and rats) could die during and after CCAO or CCAS, in that severe brain damages as well as cardiac arrests were induced by the operation (*Crespo-Garcia et al., 2018; Venkat, Chopp & Chen, 2015; Wellons Iii et al., 2000; Yang et al., 1997*). This evokes several matters such as unexpected loss and individual variations of experimental models. Furthermore, severe brain injuries have changes to cause retinal damages directly (termed as “retrograde degeneration”) (*Venkat, Chopp & Chen, 2015*), not by retinal ischemia itself.

In this regard, we previously established a stable mouse model of retinal ischemia induced by unilateral CCAO (UCCAO) with 100% survival rate during and after the operation through minimization of brain damages and showed time courses of common ischemic findings in the unilateral retina (*Lee et al., 2020a*), which were generally seen in other CCAO and CCAS models (*Crespo-Garcia et al., 2018; Davidson et al., 2000; Lavinsky et al., 2006; Lee et al., 2020b; Ogishima et al., 2011; Qin et al., 2019; Sun et al., 2019; Venkat, Chopp & Chen, 2015; Wellons Iii et al., 2000; Yamamoto et al., 2006; Yang et al., 1997*). However, time courses of retinal functional changes and acute retinal injuries in this model have not been clearly studied. In this current study, we attempted to evaluate time-dependent changes in retinal function after UCCAO using electroretinography (ERG). Moreover, we investigated acute alterations by retinal ischemia such as retinal thinning, gliosis and cell death after UCCAO with time courses using optical coherence tomography (OCT), immunohistochemistry and TUNEL assay, respectively.

## MATERIALS & METHODS

### Animal

Adult mice (male C57BL6, 6–8 weeks old,  $n = 42$ ) were purchased from CLEA Japan (Tokyo, Japan) and they were maintained in a temperature ( $24 \pm 1$  °C)-controlled environment (5–6 mice per cage) under a 12 h light-dark cycle. They were given ad libitum access to food and water. Any sign of diseases were constantly checked every day. All animal experimental protocols were approved by Keio University School of Medicine IACUC (Institutional Animal Care and Use Committees, approved number: #16017), and all experiments were carried out in accordance with the international standards of animal care and use in the ARVO (Association for Research in Vision and Ophthalmology) Statement for the Use of Animals in Ophthalmic and Vision Research.

### Unilateral common carotid artery occlusion (UCCAO)

UCCAO was conducted as previously described ([Lee et al., 2020a](#)) with a minor modification regarding an anesthetic technique. We assigned 21 mice for UCCAO and age-matched 21 mice for a sham surgery. After randomization of 42 mice without any special restrictions, they were individually anesthetized by intraperitoneal injection with a combination of MMB (midazolam, medetomidine and butorphanol tartrate) as previously described ([Miwa, Tsubota & Kurihara, 2019b](#); [Tomita et al., 2020](#)). After anesthesia, the right CCA was occluded clearly by two 6–0 silk sutures and cut between the two ties by a surgical scissor. After the operation, mice were recovered quickly by intraperitoneal injection with a solution of atipamezole hydrochloride as previously described ([Miwa, Tsubota & Kurihara, 2019b](#); [Tomita et al., 2019](#)). For the management of pain, 0.4 mg/kg of butorphanol tartrate was injected to mice when mice woke up ([Lee et al., 2020b](#)). For a sham surgery, mice underwent the same step except for the occlusion. At the end of all the experiments or during the experiments in which signs such as hunched posture, lethargy, lack of food intake or infection of the surgery site were seen in mice, a combination of 3x of MMB was injected to mice ([Lee et al., 2020b](#)) and then mice were euthanized under deep anesthesia.

### Electroretinography (ERG)

ERG was set and conducted using a Ganzfeld dome, PuREC acquisition system and LED stimulators by a blinded investigator as previously described ([Miwa, Tsubota & Kurihara, 2019b](#); [Tomita et al., 2019](#)). Following dark adaptation more than 12 h, mice were anesthetized by intraperitoneal injection with a combination of MMB under dim red light in a dark room. The pupils were dilated by a solution of 0.5% tropicamide and 0.5% phenylephrine. The active electrodes were touched on contact lens and the reference electrode was inserted into the mouth. Scotopic responses were recorded with various intensities of stimuli under dim red light in a dark room. Heat pads were prepared to keep all mice warm during the procedure. The amplitude of a-wave was calculated from the baseline to the lowest point of a-wave and the amplitude of b-wave was calculated from the lowest point of a-wave to the peak of b-wave. The amplitudes of oscillatory potentials (OPs) were measured at the four peaks of OPs as previously described ([Tomita et al., 2020](#)).

When the electrodes were detached from contact lens of mice by unexpected movements of the electrodes during the experiments, data points were marked and excluded for further analyses. Except for this issue, all data points from the experiments were included for further analyses. Confounders were not controlled as experiments were processed randomly and individually.

### **Immunohistochemistry**

The eyes fixed in 4% PFA-added tubes for 24 h were incubated with 10–30% sucrose on ice until the eyes dropped to the bottom of the tubes. O.C.T. Compound (Sakura Tissue-Tek, Tokyo, Japan) was used to quickly embed the eyes for frozen sectioning. Cryostat (Leica CM3050S, Leica, Wetzlar, Germany) was conducted to obtain sagittal sectioning slides of the eyes. The sagittal sectioning slides were washed with PBS three times and then incubated in blocking solution (PBS + 0.1% Triton + 0.1% BSA) for 1 h at room temperature. The retinas were incubated with a primary antibody (GFAP 1:400, Cat #13-0300, Thermo Fisher Scientific, USA) overnight at 4 °C. The retinas were washed with PBS + 0.1% Triton several times and incubated with a species-appropriate fluorescence-conjugated secondary antibody (Thermo Fisher Scientific, USA) for 2 h at room temperature in a dark room. After washing with PBS + 0.1% Triton three times, DAPI was incubated for 1 min in order to stain nuclei. After washing with PBS three times, the retinas were mounted and examined via a fluorescence microscope (LSM710, Carl Zeiss, Jena, Germany), as previously described ([Lee et al., 2020b](#)). The fluorescence immunoreactivity was quantified by a morphology score as previously described ([Lee et al., 2020a](#); [Yamamoto et al., 2006](#)) with a minor modification: 0 = no signal, 1 = labelled processes in the ganglion cell layer, 2 = labelled processes in the inner retinal layer including the ganglion cell layer, and 3 = labelled processes in the entire retinal layer including the inner and outer retinas.

### **TUNEL assay**

Sagittal sectioning slides of the eyes were subjected to TUNEL assay. The assay was conducted following the manufacturer's instruction (in situ Apoptosis Detection Kit, Cat #MK500, Takara Bio, Japan). Briefly, the slides were washed with PBS three times. Permeabilization buffer was applied to the slides for 5 min on ice. After washing with PBS three times, labeling reaction mixture containing TdT enzymes were applied to the samples for 1 h. After washing with PBS three times, DAPI was added for 1 min to stain nuclei. After washing with PBS three times, the slides were mounted and examined via a fluorescence microscope (LSM710; Carl Zeiss, Jena, Germany).

### **Optical coherence tomography (OCT)**

We performed OCT (Envisu R4310, Leica, Wetzlar, Germany) as previously described ([Miwa et al., 2019a](#)). Briefly, a combination of 0.5% tropicamide and 0.5% phenylephrine (Santen Pharmaceutical, Osaka, Japan) was added to mice for 5 min for induction of mydriasis. Anesthetized mice by a combination of MMB were placed in an OCT platform and then OCT was immediately conducted. 0.2, 0.4 and 0.6 mm from the optic nerve head in the retina were marked. Then, total retinal thickness (from the outer retina to the inner

retina including the ganglion cell layer) was measured via OCT software (Envisu R4310, Leica, Wetzlar, Germany).

### Statistical analysis

Analyses of data from the experiments were conducted with GraphPad Prism 5 (USA). All values in data were presented as mean  $\pm$  standard deviation. Statistical significance was calculated by using a two-tailed Student's *t*-test or a two-way ANOVA followed by a Bonferroni post hoc test, and *p*-value of less than 0.05 was considered to be significant statistically.

## RESULTS

### Decreases in the amplitudes of a- and b-waves after UCCAO

We examined whether retinal function could be altered 3 days after UCCAO (Fig. 1). The amplitudes of a- and b-waves were not significantly different between the UCCAO-operated mice and the sham-operated mice. There was an only slight decrease in the amplitude of b-wave in the UCCAO-operated right eye in comparison with that of b-wave in the sham-operated right eye.

Next, retinal function was further examined 7 days after UCCAO (Fig. 2). We found a significant decrease in the amplitude of b-wave in the UCCAO-operated right eye, in comparison with that of b-wave in the sham-operated right eye. There was a decreasing tendency with significance in the amplitude of a-wave in the UCCAO-operated right eye, in comparison with that of a-wave in the sham-operated right eye. When it comes to the left eye, we could not find a significant alteration in retinal function after UCCAO.

On day 14 after UCCAO, we could more clearly see a dramatic decrease in the amplitudes of both a- and b-waves in the UCCAO-operated right eye, in comparison with those of waves in the sham-operated right eye (Fig. 3). We still could not find a significant alteration in left retinal function after UCCAO.

### Decreases in the amplitudes of OPs after UCCAO

As retinal dysfunction in the right eye was observable clearly on day 14 after UCCAO, we further examined retinal dysfunction using another value, "OPs" (Fig. 4). The reduced amplitudes of OPs are known to occur in various types of murine and human retinopathies (Crespo-Garcia et al., 2018; Davidson et al., 2000; Hancock & Kraft, 2004; Kizawa et al., 2006; Kurihara et al., 2008; Li et al., 2002; Qin et al., 2019; Shirao & Kawasaki, 1998; Tomita et al., 2019). Reduction in OP1, OP2, OP3, OP4 and total OPs ( $\Sigma$ OPs) amplitudes was observed in the UCCAO-operated right eye, in comparison with that in the sham-operated right eye. There was no significant difference in the amplitudes between the sham and UCCAO-operated left eyes.

### A transient decrease in the amplitude ratio of b/a wave after UCCAO

After ERG analyses, we retrospectively calculated the b/a wave amplitude ratio (low and high intensities: 0.1 and 10 cd s/m<sup>2</sup>) on day 3, 7 and 14 (Fig. 5). The significantly decreased ratio in the UCCAO-operated right eye was seen on day 7 after UCCAO. The decreased

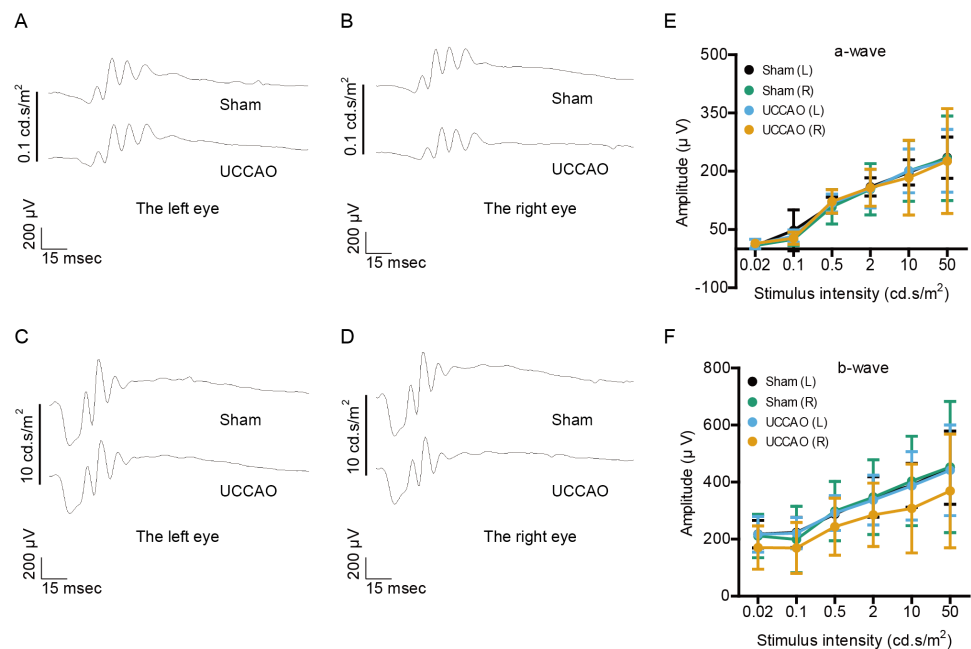


**Figure 1** Any change in retinal function is not seen on day 3 after UCCAO. (A–D) Representative waveforms of a- and b-waves (low and high intensities, 0.1 and 10 cd s/m<sup>2</sup>, respectively) of the right and left eyes in the sham- and UCCAO-operated mice ( $n = 8$  for UCCAO-operated group and 8 for sham-operated group) and (E–F) quantitative analyses showed that the amplitudes of a- and b-waves were not significantly different among all of the eyes in sham- and UCCAO-operated mice 3 days after the operation. Graphs were presented as mean  $\pm$  standard deviation. The data were analyzed using a two-tailed Student's  $t$ -test.  $P > 0.05$ . Black (sham L), the sham-operated left eye; bluish green (sham R), the sham-operated right eye; sky blue (UCCAO L), the UCCAO-operated left eye; orange (UCCAO R), the UCCAO-operated right eye.

Full-size DOI: 10.7717/peerj.11665/fig-1

b/a wave amplitude ratio returned to the range similar to the range in the sham-operated eye on day 14 after UCCAO.

### Observation in retinal thickness changes after UCCAO

We further examined whether retinal thickness could be changed by UCCAO. Although there was slight fluctuation in retinal thickness for 14 days after UCCAO, we could not detect a significant change in total retinal thickness for 14 days after UCCAO (Fig. 6). During the experimental period, only one mouse showed a severe cataract; therefore retinal thickness in this mouse could not be measured by OCT.

### Retinal gliosis and cell death after UCCAO

We examined whether retinal gliosis and retinal cell death could be induced by UCCAO. Acute retinal gliosis has been reported in this model (Lee et al., 2020a). We could also detect this finding on day 3, analyzed by a higher morphology score in the right retina after UCCAO, compared with that in the sham-operated right retina (Fig. 7). This finding was maintained for 14 days after UCCAO (Fig. 7). When it comes to retinal cell death, even though we could not detect TUNEL (+) cells in the retina on day 3 and 14, TUNEL (+) cells were substantially detected in the right retina on day 7 after UCCAO (Fig. 8).



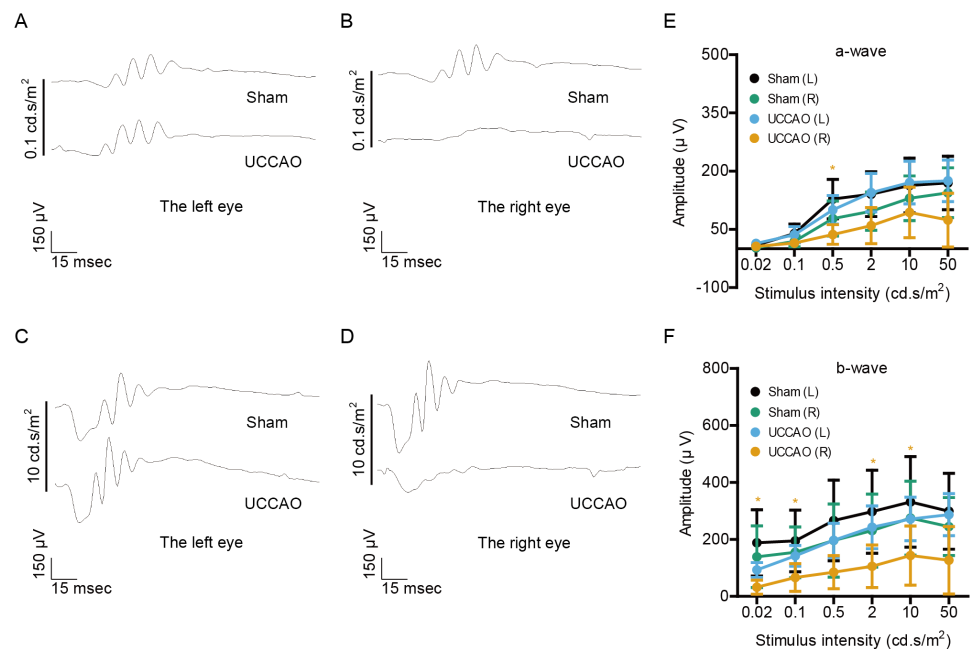


**Figure 2** Changes in retinal function are seen on day 7 after UCCAO. (A–D) Representative waveforms of a- and b-waves (low and high intensities, 0.1 and 10 cd.s/m<sup>2</sup>, respectively) of the right and left eyes in sham- and UCCAO-operated mice ( $n = 8$  for UCCAO-operated group and 8 for sham-operated group) and (E–F) quantitative analyses showed that the amplitude of b-wave dramatically decreased in the UCCAO-operated unilateral right eye, in comparison with that in the sham-operated right eye 7 days after the operation. Graphs were presented as mean  $\pm$  standard deviation. The data were analyzed using a two-tailed Student's  $t$ -test. \*  $P < 0.05$ . Black (sham L), the sham-operated left eye; bluish green (sham R), the sham-operated right eye; sky blue (UCCAO L), the UCCAO-operated left eye; orange (UCCAO R), the UCCAO-operated right eye.

Full-size [DOI: 10.7717/peerj.11665/fig-2](https://doi.org/10.7717/peerj.11665/fig-2)

## DISCUSSION

The present study was designed to evaluate whether UCCAO-induced ischemic stresses in the retina could contribute to the development of retinal dysfunction and acute retinal injuries. Based on previous data, UCCAO has been suggested to cause abnormalities in retinal blood flow, stabilization of hypoxia-inducible factor-1  $\alpha$  (HIF-1  $\alpha$ ) and HIF-2  $\alpha$  in the unilateral retina, induction of hypoxia-responsive genes including hypoxia-induced inflammatory cytokines, acute retinal reactive gliosis and chronic inner retinal thinning (Lee et al., 2019; Lee et al., 2020a; Lee et al., 2021). Although several retinal ischemic findings were unraveled in this model, there were missing points, especially retinal functional changes and acute retinal injuries. In this current study, we firstly demonstrated functional impairment in the retina could gradually occur from 3 days to 7 days after the occlusion and its impairment could be clearly observed 14 days after the occlusion. Furthermore, its functional deficit could be explained with acute retinal cell death as well as continuous retinal gliosis by the occlusion, which is a significance of our study.

ERG recordings were used in order to evaluate retinal functional changes by UCCAO. a-wave provides functional status of photoreceptors (Brown, 1968; Robson et al., 2003),

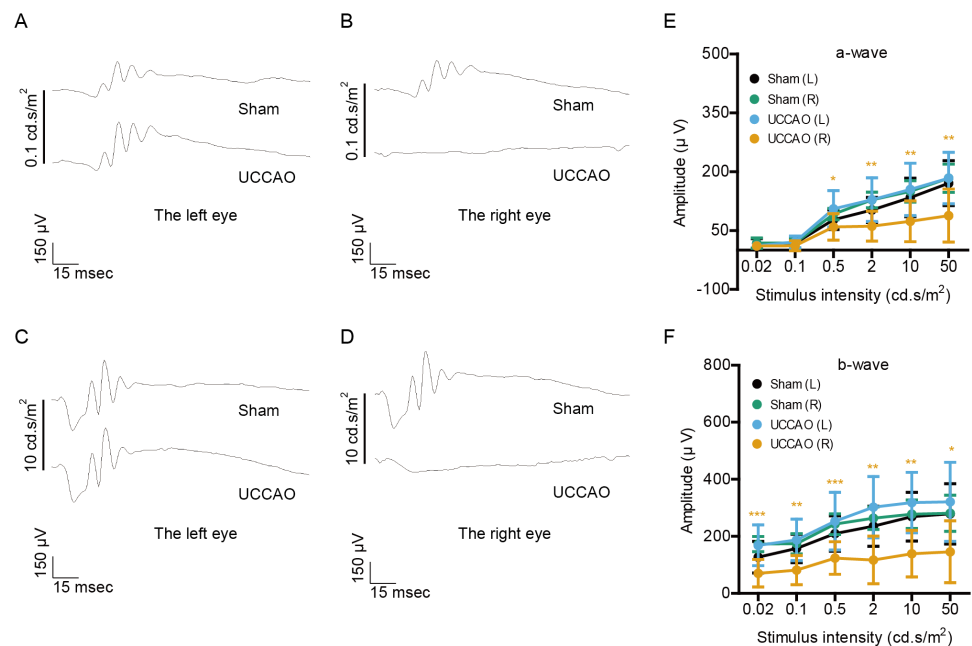


**Figure 3** Changes in retinal function are clearly seen on day 14 after UCCAO. (A–D) Representative waveforms of a- and b-waves (low and high intensities, 0.1 and 10 cd s/m<sup>2</sup>, respectively) of the right and left eyes in sham- and UCCAO-operated mice ( $n = 8$  for UCCAO-operated group and 8 for sham-operated group) and (E–F) quantitative analyses showed that the amplitudes of a- and b-waves significantly and dramatically decreased in the UCCAO-operated unilateral right eye, in comparison with those in the sham-operated right eye 14 days after the operation. Graphs were presented as mean  $\pm$  standard deviation. The data were analyzed using a two-tailed Student's  $t$ -test. \*  $P < 0.05$ , \*\*  $P < 0.01$ , \*\*\*  $P < 0.001$ . Black (sham L), the sham-operated left eye; bluish green (sham R), the sham-operated right eye; sky blue (UCCAO L), the UCCAO-operated left eye; orange (UCCAO R), the UCCAO-operated right eye.

Full-size [DOI: 10.7717/peerj.11665/fig-3](https://doi.org/10.7717/peerj.11665/fig-3)

whereas b-wave provides conditions on functional activities of Müller cells and/or bipolar cells (Miller & Dowling, 1970). Moreover, cellular origins of OPs are neurons in the inner retinal layer such as bipolar and amacrine cells (Heynen, Wachtmeister & Van Norren, 1985; Wachtmeister, 1998; Yonemura & Kawasaki, 1979). We found that the amplitude of b-wave was more affected than that of a-wave by UCCAO, and the amplitudes of OPs dramatically became lower. In our previous data and present data, reactive gliosis in Müller cells and astrocytes, which is activated under ocular ischemic conditions (Vecino et al., 2016), was mostly detected in the inner retina layer among the whole retinal layers after UCCAO (Lee et al., 2020a). Retinal cell death was more observable in the inner retina 7 days after UCCAO. Even though there was no acute change in retinal thickness, inner retinal thinning was observed more than the outer retinal thinning after UCCAO at the chronic stage, 10 weeks after UCCAO (Lee et al., 2020a). A pathological change in other CCAO and CCAS models was also a decrease in thickness of the inner retinal layer (Crespo-Garcia et al., 2018; Kalesnykas et al., 2008; Lavinsky et al., 2006; Ogishima et al., 2011; Qin et al., 2019; Sun et al., 2019; Yamamoto et al., 2006). With this together, carotid artery occlusion-induced retinal ischemic models seem applicable to study pathological mechanisms of functional



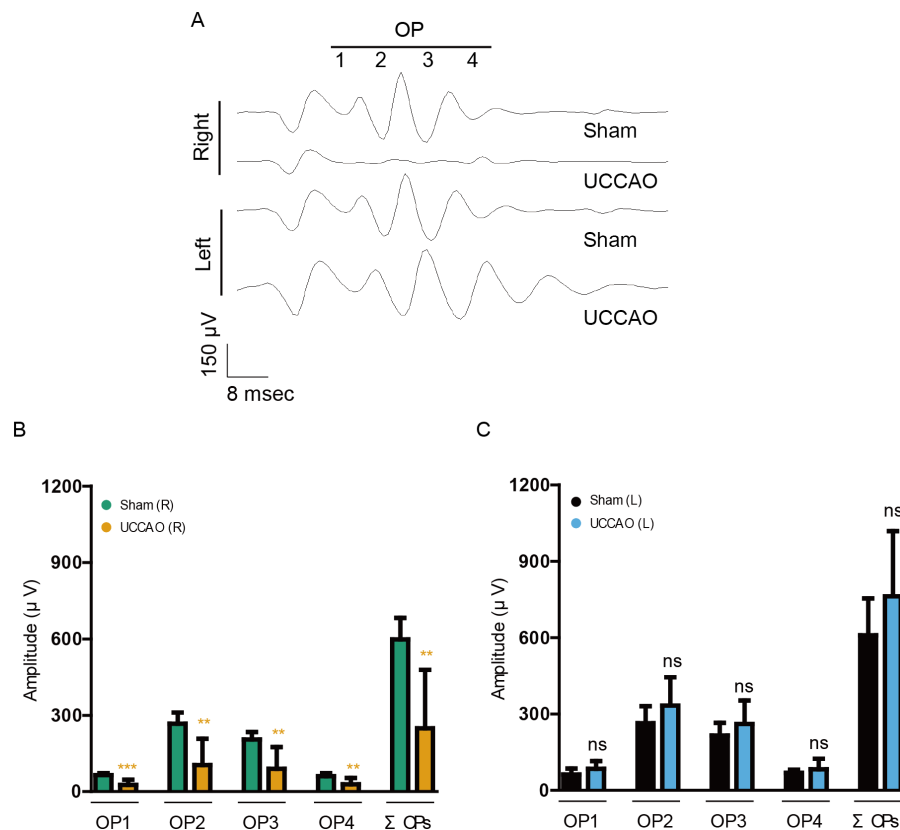


**Figure 4** A reduction in the amplitudes of OPs is seen on day 14 after UCCAO. (A) Representative waveforms of OPs of the right and left eyes in the sham- and UCCAO-operated mice ( $n = 8$  for UCCAO-operated group and 8 for sham-operated group) and (B–C) quantitative analyses showed that the amplitudes of OPs significantly decreased in the UCCAO-operated unilateral right eye, in comparison with those in the sham-operated eye 14 days after the operation. Graphs were presented as mean  $\pm$  standard deviation. The data were analyzed using Student's *t*-test. \*\*  $P < 0.01$ , \*\*\*  $P < 0.001$ . Black (sham L), the sham-operated left eye; bluish green (sham R), the sham-operated right eye; sky blue (UCCAO L), the UCCAO-operated left eye; orange (UCCAO R), the UCCAO-operated right eye. OP, oscillatory potential.

Full-size [DOI: 10.7717/peerj.11665/fig-4](https://doi.org/10.7717/peerj.11665/fig-4)

and histological ischemic damages in the inner retinal layer at the chronic stage. However, UCCAO also damages the outer retinal layer, analyzed by retinal gliosis in the entire retinal layer, retinal cell death in the outer retina and a reduction in the amplitude of a-wave after UCCAO with a transient decrease in the amplitude ratio of b/a wave. This can be explained by the fact that vessels supplying the outer retina and the inner retina are originated from the same internal carotid artery, one of two branches of the common carotid artery. Anatomical ocular circulation is needed to be taken into account for deep understanding of inner and outer retinal ischemic damages by UCCAO. Therefore, a comparison analysis on damaging intensities between the outer and the inner retinas along with alterations in ocular circulation (choroid and retinal circulation) by UCCAO will be further studied.

Even though this mouse model shows common retinal ischemic injuries, several limitations for interpretation of the current outcomes exist. Compared to murine models of bilateral common carotid artery occlusion and stenosis (Kalesnykas et al., 2008; Lavinsky

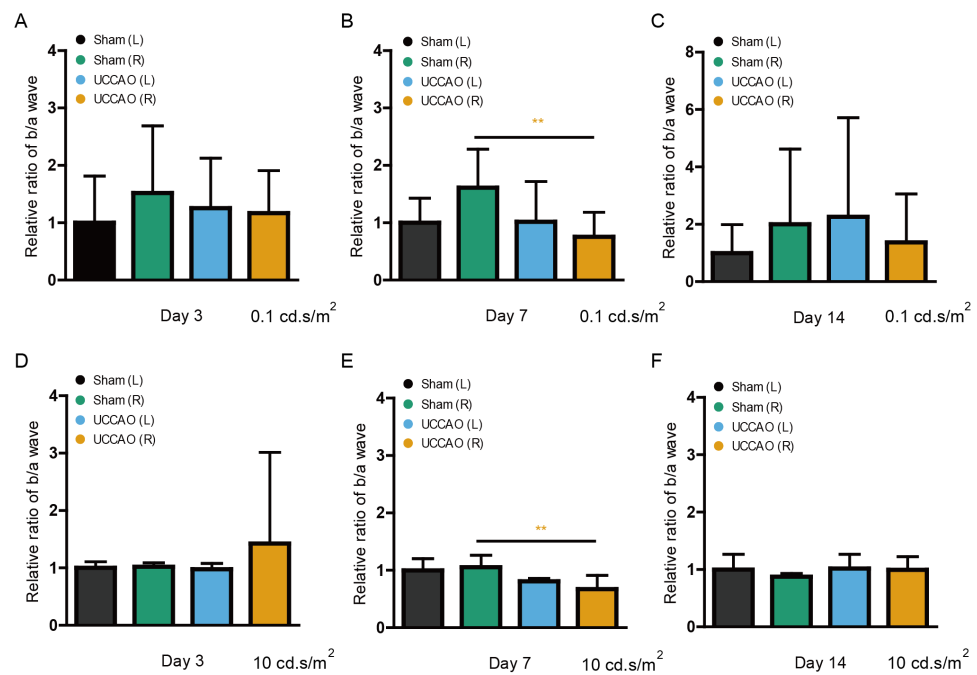


**Figure 5** A transient reduction in the amplitude ratio of b/a wave is seen after UCCA O. (A–F) Quantitative analyses based on the values of the amplitude ratio of b/a wave from Fig. 1 to Fig. 3 (low and high intensities, 0.1 and 10 cd s/m<sup>2</sup>, respectively) showed that its ratio significantly decreased in the UCCA O-operated unilateral right eye, in comparison with that in the sham-operated eye only on day 7 after the operation. Graphs were presented as mean  $\pm$  standard deviation. The data were analyzed using Student's *t*-test. \*\*  $P < 0.01$ . Black (sham L), the sham-operated left eye; bluish green (sham R), the sham-operated right eye; sky blue (UCCA O L), the UCCA O-operated left eye; orange (UCCA O R), the UCCA O-operated right eye.

Full-size DOI: 10.7717/peerj.11665/fig-5

*et al.*, 2006; Qin *et al.*, 2019; Sun *et al.*, 2019; Yamamoto *et al.*, 2006), milder retinal ischemic stress is observed in this UCCA O model. In this regard, retinal thinning was not dramatically observed in a short-term period even though there was retinal cell death. In fact, retinal cell death in this UCCA O model is also seen weaker than that in other retinal injury models (Luo *et al.*, 2020; Matei *et al.*, 2020; Song *et al.*, 2008). Long-term period studies may be necessary to observe histological injuries in the retina by UCCA O. However, this milder effect could be more relevant to study ischemic retinopathies in human, in that retinal ischemic injuries in human are gradually induced with time (Terelak-Borys, Skonieczna & Grabska-Liberek, 2012). Even though our current data showed retinal cell death in the outer and inner retina, what kinds of cells are damaged after UCCA O has not been deeply studied. Therefore, co-labeling of TUNEL with specific retinal cell markers is needed to expand understanding of retinal cell death depending on the cell types by UCCA O, which will be further studied. Next, metabolic complications have been closely associated with the development of human ischemic retinopathies such as ocular ischemic syndrome or diabetic retinopathies (Sim *et al.*, 2013). Such metabolic complications have not been applied to this model in this study. Therefore, the ischemic processes from this model may not be directly corresponded with the development of human ischemic retinopathies. Nonetheless, this issue could be solved

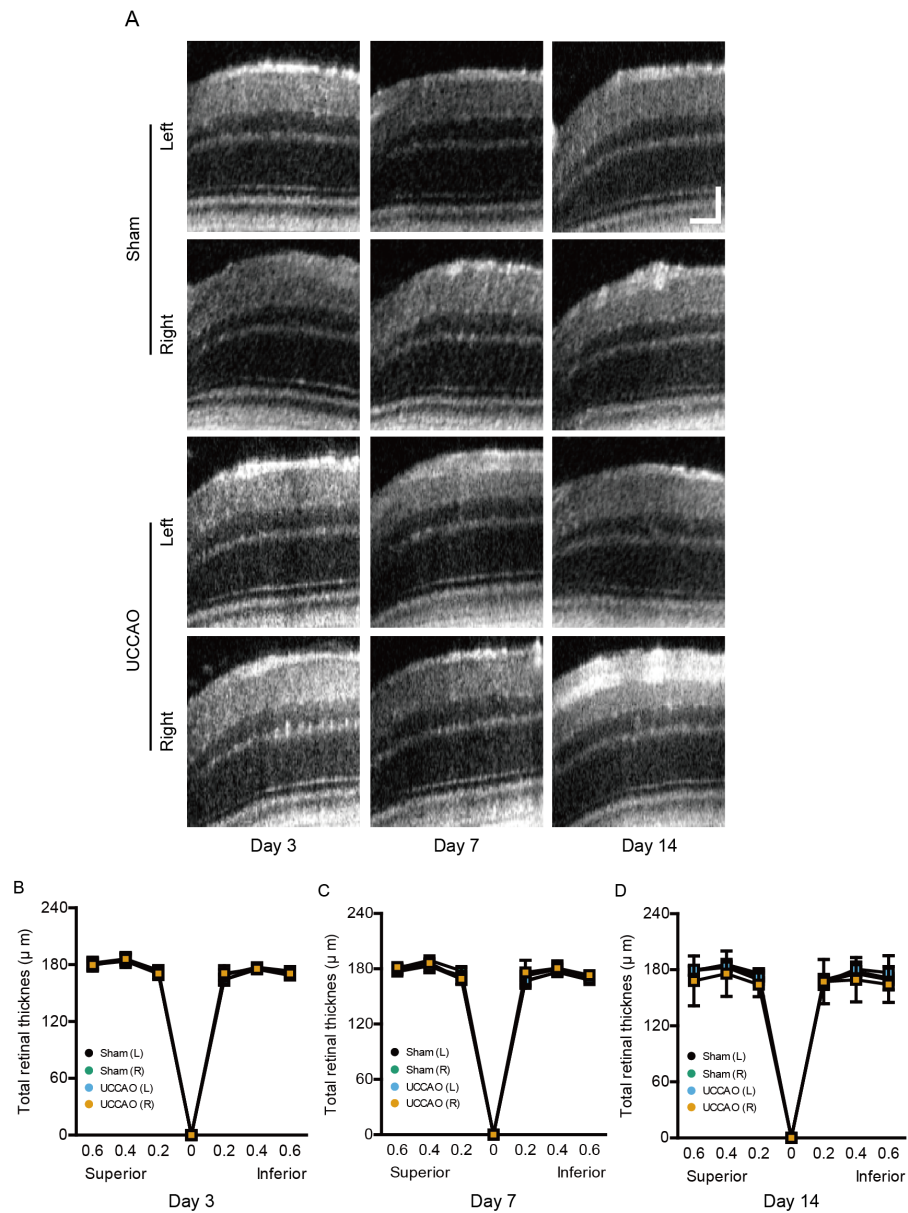


**Figure 6** A dramatic change in retinal thickness is not detected for 14 days after UCCAO. (A) Representative OCT images in the sham- and UCCAO-operated retinas and (B–D) quantitative analyses showed that there was no change in retinal thickness in the right and left eyes in the sham- and UCCAO-operated mice ( $n = 6–7$  for UCCAO-operated group and  $6–7$  for sham-operated group) for 14 days after the operation. Horizontal scale bar:  $100 \mu\text{m}$ ; Vertical scale bar:  $50 \mu\text{m}$ .  $P > 0.05$ . The values in the horizontal axis of spider diagrams represent 0.2, 0.4 and 0.6 mm distant from the optic nerve head (0). The measurement site in the representative example images was  $400 \mu\text{m}$  from the optic nerve head. The data were analyzed using two-way ANOVA followed by a Bonferroni post hoc test. Spider diagrams were presented as mean with  $\pm$  standard deviation. Black (sham L), the sham-operated left eye; bluish green (sham R), the sham-operated right eye; sky blue (UCCAO L), the UCCAO-operated left eye; orange (UCCAO R), the UCCAO-operated right eye.

Full-size DOI: [10.7717/peerj.11665/fig-6](https://doi.org/10.7717/peerj.11665/fig-6)

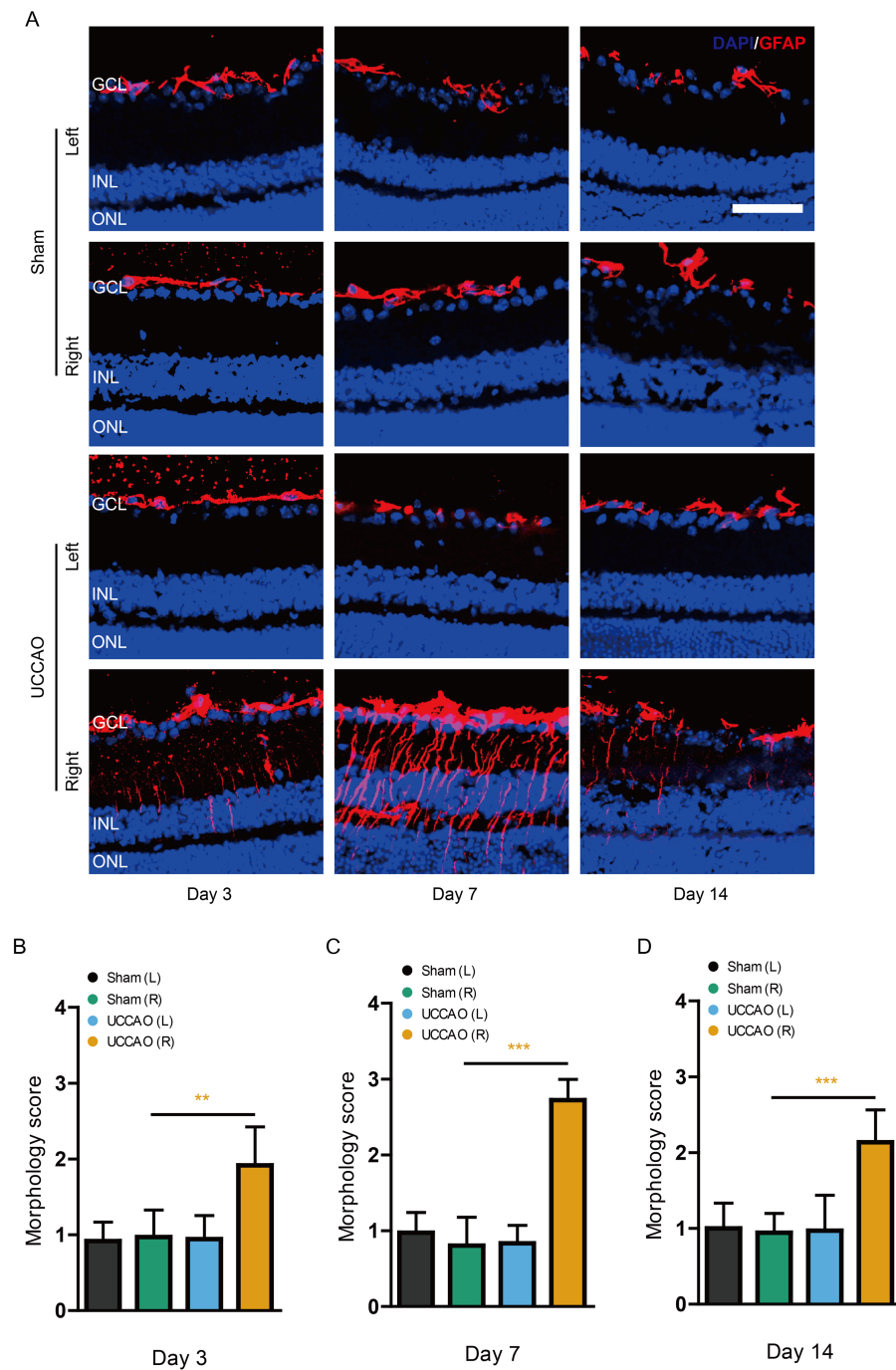


**Figure 7** Retinal gliosis is continuously observed for 14 days after UCCA. (A) Representative images and (B–D) quantitative analyses showed that there was retinal gliosis stained by GFAP in the right retina in the UCCA-operated mice ( $n = 6$  for UCCA-operated group and 6 for sham-operated group) for 14 days after the operation. Scale bar: 50  $\mu\text{m}$ . Graphs were presented as mean with  $\pm$  standard deviation. The data were analyzed using Student's  $t$ -test. \*\*  $P < 0.01$ , \*\*\*  $P < 0.001$ . Black (sham L), the sham-operated left eye; bluish green (sham R), the sham-operated right eye; sky blue (UCCA L), the UCCA-operated left eye; orange (UCCA R), the UCCA-operated right eye. GCL, ganglion cell layer; INL, inner retinal layer; ONL, outer retinal layer.

Full-size DOI: 10.7717/peerj.11665/fig-7

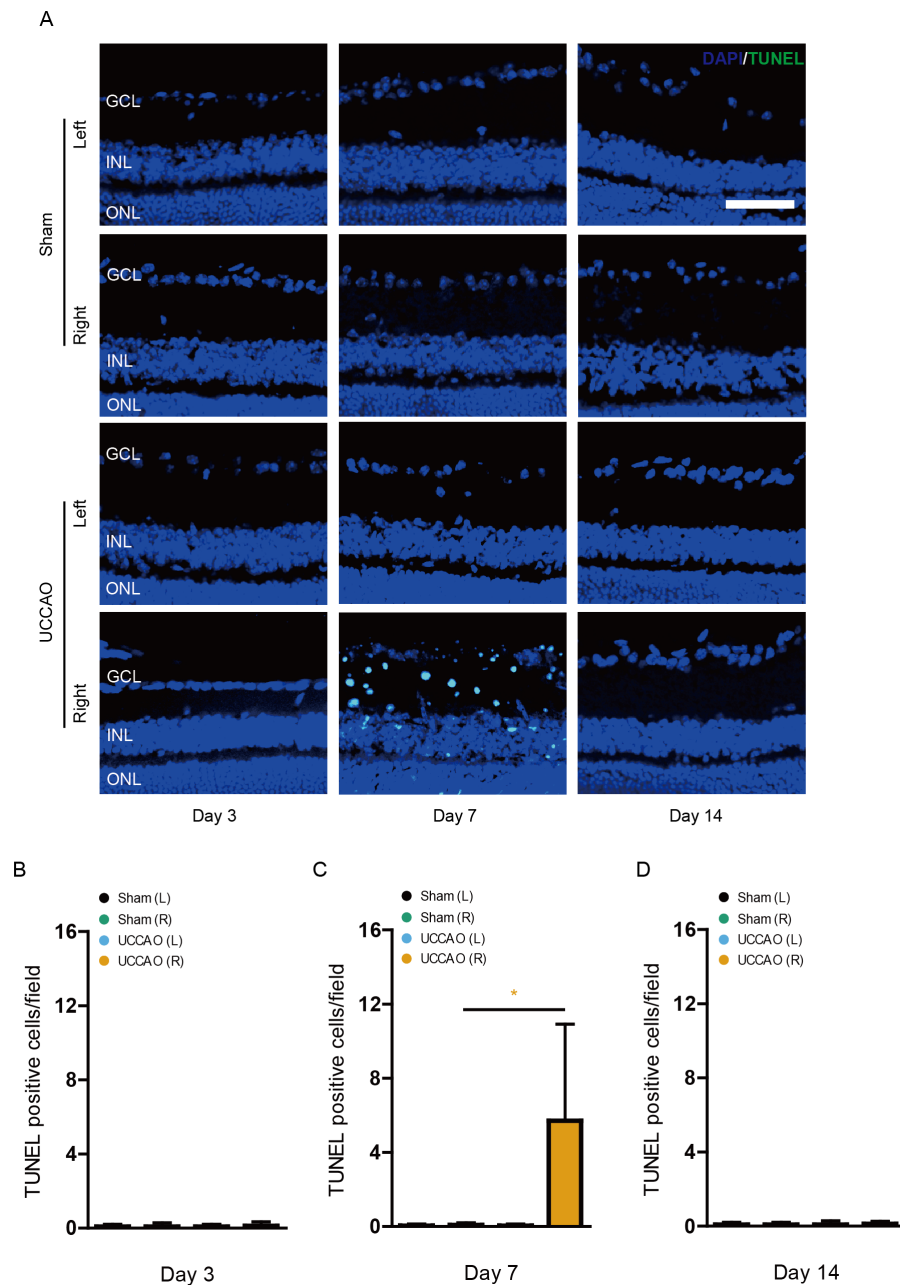


**Figure 8** Retinal cell death is observed on day 7 after UCCA O. (A) Representative images and (B-D) quantitative analyses showed that there were TUNEL (+) cells in the right retina in the UCCA O-operated mice ( $n = 6$  for UCCA O-operated group and 6 for sham-operated group) only 7 days after the operation. Scale bar:  $50 \mu\text{m}$ . Graphs were presented as mean with  $\pm$  standard deviation. The data were analyzed using Student's  $t$ -test. \*  $P < 0.05$ . Black (sham L): the sham-operated left eye; bluish green (sham R): the sham-operated right eye; sky blue (UCCA O L): the UCCA O-operated left eye; orange (UCCA O R): the UCCA O-operated right eye. GCL: ganglion cell layer; INL: inner retinal layer; ONL: outer retinal layer.

Full-size [DOI: 10.7717/peerj.11665/fig-8](https://doi.org/10.7717/peerj.11665/fig-8)

with combination of murine models of metabolic diseases such as diabetes (genetically diabetic db/db mice and/or streptozotocin-induced diabetic mice) with UCCAO. With this approach, we can develop more clinically relevant murine models of ischemic retinopathies. Next, we selected MMB (midazolam, medetomidine and butorphanol tartrate) for the surgery as well as OCT and ERG recordings. MMB has been widely used as a favorable anesthetic in experimental models since ketamine was enrolled as a narcotic drug in Japan in 2007 ([Kawai et al., 2011](#); [Kirihara et al., 2019](#)). Even though all mice received the same anesthetic procedure in this study, it may be important to deeply consider appropriate anesthetics and time of anesthesia for the surgery as well as OCT and ERG recordings.

In our current study, we found that only the right (ipsilateral) eye was dramatically damaged by UCCAO. When it comes to the left (contralateral) eye, there was no significant difference in the retinal ischemic outcomes between the sham- and UCCAO-operated mice. As the left retina can be considered as a control for the right retina, we can minimize the number of experimental animals for further other studies such as *in vivo* drug screenings or knock-out mouse work which needs substantial handling and breeding of mice. Moreover, UCCAO model can reduce inter-individual differences. Substantial inter-individual variabilities are not evitable even though genetically identical experimental mice are used for experimental studies ([Freund et al., 2013](#); [Van Dongen et al., 2012](#)). In this regard, this UCCAO model has a strong benefit for comparison analyses by using left and right eyes in the same individual animals. This implies a reduction in variations of retinal and circulatory conditions of each animal and other variable factor such as diet and oxygen consumption. However, more studies may be required for using the left (contralateral) retina as a control in that unexpected compensation signals from the right (ipsilateral) ischemic retinal damages (which we have not found yet) might occur in the left (contralateral) retina.

## CONCLUSIONS

In conclusion, along with previous findings in this model ([Lee et al., 2019](#); [Lee et al., 2020a](#); [Lee et al., 2021](#)), we have demonstrated exact time courses of pathological dysfunction, continuous reactive gliosis and transient cell death in the unilateral retina after UCCAO in mice. After UCCAO, retinal blood flow becomes abnormal, leading to retinal ischemia confirmed by stabilization of HIF-1  $\alpha$  and HIF-2  $\alpha$  with induction of hypoxia-responsive genes and hypoxia-induced inflammatory cytokines. Next, acute reactive gliosis and cell death in the retina occurs and retinal function decreases at the early stage. Finally, the inner retinal layer becomes thinner with reduction in inner retinal cell maker gene expressions at the chronic stage.

We suggest that this model could be useful as a stable experimental model for the study of adult retinal ischemia and it will present an experimental ground for the further investigation of the pathogenesis for human retinal ischemic injuries.

## ACKNOWLEDGEMENTS

The authors thank S. Ikeda, K. Kurosaki and A. Kawabata for critical discussions.



## ADDITIONAL INFORMATION AND DECLARATIONS

### Funding

This work was supported by Grants-in-Aid for Scientific Research (KAKENHI) (18K09424 to Toshihide Kurihara). The funders had no role in study design, data collection and analysis, decision to publish, or preparation of the manuscript.

### Grant Disclosures

The following grant information was disclosed by the authors:  
Scientific Research (KAKENHI): 18K09424.

### Competing Interests

Yukihiro Miwa is employed by Tokyo Animal Eye Clinic and Kazuo Tsubota is employed by Tsubota Laboratory, Inc. The other authors declare that they have no competing interests.

### Author Contributions

- Deokho Lee conceived and designed the experiments, performed the experiments, analyzed the data, prepared figures and/or tables, authored or reviewed drafts of the paper, and approved the final draft.
- Heonuk Jeong performed the experiments, analyzed the data, prepared figures and/or tables, authored or reviewed drafts of the paper, and approved the final draft.
- Yukihiro Miwa, Ari Shinojima and Yusaku Katada performed the experiments, prepared figures and/or tables, critical discussion, and approved the final draft.
- Kazuo Tsubota and Toshihide Kurihara conceived and designed the experiments, authored or reviewed drafts of the paper, supervision, and approved the final draft.

### Animal Ethics

The following information was supplied relating to ethical approvals (i.e., approving body and any reference numbers):

All animal experimental protocols were approved by Keio University School of Medicine IACUC (Institutional Animal Care and Use Committees), and all experiments were carried out in accordance with the international standards of animal care and use in the ARVO (Association for Research in Vision and Ophthalmology) Statement for the Use of Animals in Ophthalmic and Vision Research.

Approved number #16017.

### Data Availability

The following information was supplied regarding data availability:

The raw measurements are available in the [Supplemental File](#).

### Supplemental Information

Supplemental information for this article can be found online at <http://dx.doi.org/10.7717/peerj.11665#supplemental-information>.

## REFERENCES

- Brown KT. 1968.** The electroretinogram: its components and their origins. *Vision Research* 8:633–677 DOI 10.1016/0042-6989(68)90041-2.
- Chou C-C, Hsu M-Y, Lin C-H, Lin C-C, Wang C-Y, Shen Y-C, Wang IJ. 2018.** Risk of developing open-angle glaucoma in patients with carotid artery stenosis: a nationwide cohort study. *PLOS ONE* 13:e0194533 DOI 10.1371/journal.pone.0194533.
- Crespo-Garcia S, Reichhart N, Skosyrski S, Foddiss M, Wu J, Figura A, Herrspiegel C, Fuchtemeier M, Sassi C, Dirnagl U, Joussem AM, Strauss O. 2018.** Individual and temporal variability of the retina after chronic bilateral common carotid artery occlusion (BCCAO). *PLOS ONE* 13(3):e0193961 DOI 10.1371/journal.pone.0193961.
- Dattilo M, Newman NJ, Bioussé V. 2018.** Acute retinal arterial ischemia. *Annals of Eye Science* 3:28 DOI 10.21037/aes.2018.05.04.
- Davidson CM, Pappas BA, Stevens WD, Fortin T, Bennett SAL. 2000.** Chronic cerebral hypoperfusion: loss of pupillary reflex, visual impairment and retinal neurodegeneration. *Brain Research* 859:96–103 DOI 10.1016/S0006-8993(00)01937-5.
- Drinkwater JJ, Davis TME, Davis WA. 2020.** The relationship between carotid disease and retinopathy in diabetes: a systematic review. *Cardiovascular Diabetology* 19:54 DOI 10.1186/s12933-020-01023-6.
- Faries PL, Chaer RA, Patel S, Lin SC, De Rubertis B, Kent KC. 2006.** Current management of extracranial carotid artery disease. *Vasc Endovascular Surg* 40:165–175 DOI 10.1177/153857440604000301.
- Fouda AY, Eldahshan W, Narayanan SP, Caldwell RW, Caldwell RB. 2020.** Arginase pathway in acute retina and brain injury: therapeutic opportunities and unexplored avenues. 11:277 DOI 10.3389/fphar.2020.00277.
- Freund J, Brandmaier AM, Lewejohann L, Kirste I, Kritzler M, Krüger A, Sachser N, Lindenberger U, Kempermann G. 2013.** Emergence of individuality in genetically identical mice. *Science* 340:756–759 DOI 10.1126/science.1235294.
- Hancock HA, Kraft TW. 2004.** Oscillatory potential analysis and ERGs of normal and diabetic rats. *Investigative Ophthalmology & Visual Science* 45:1002–1008 DOI 10.1167/iovs.03-1080.
- Harris A, Chung HS, Ciulla TA, Kagemann L. 1999.** Progress in measurement of ocular blood flow and relevance to our understanding of glaucoma and age-related macular degeneration. *Progress in Retinal and Eye Research* 18:669–687 DOI 10.1016/S1350-9462(98)00037-8.
- Heynen H, Wachtmeister L, Van Norren D. 1985.** Origin of the oscillatory potentials in the primate retina. *Vision Research* 25:1365–1373 DOI 10.1016/0042-6989(85)90214-7.
- Kalesnykas G, Tuulos T, Uusitalo H, Jolkkonen J. 2008.** Neurodegeneration and cellular stress in the retina and optic nerve in rat cerebral ischemia and hypoperfusion models. *Neuroscience* 155:937–947 DOI 10.1016/j.neuroscience.2008.06.038.
- Kawai S, Takagi Y, Kaneko S, Kurosawa T. 2011.** Effect of three types of mixed anesthetic agents alternate to ketamine in mice. *Experimental Animals* 60:481–487 DOI 10.1538/expanim.60.481.

- Kirihara Y, Takechi M, Kurosaki K, Matsuo H, Kajitani N, Saito Y. 2019.** Effects of an anesthetic mixture of medetomidine, midazolam, and butorphanol and antagonism by atipamezole in rabbits. *Experimental Animals* **68**:443–452 DOI [10.1538/expanim.18-0183](https://doi.org/10.1538/expanim.18-0183).
- Kizawa J, Machida S, Kobayashi T, Gotoh Y, Kurosaka D. 2006.** Changes of oscillatory potentials and photopic negative response in patients with early diabetic retinopathy. *Japanese Journal of Ophthalmology* **50**:367–373 DOI [10.1007/s10384-006-0326-0](https://doi.org/10.1007/s10384-006-0326-0).
- Kurihara T, Ozawa Y, Nagai N, Shinoda K, Noda K, Imamura Y, Tsubota K, Okano H, Oike Y, Ishida S. 2008.** Angiotensin II Type 1 receptor signaling contributes to synaptophysin degradation and neuronal dysfunction in the diabetic retina. *Diabetes* **57**:2191 DOI [10.2337/db07-1281](https://doi.org/10.2337/db07-1281).
- Lavinsky D, Arterni NS, Sarmiento, Achaval M, Netto CA. 2006.** Chronic bilateral common carotid artery occlusion: a model for ocular ischemic syndrome in the rat. *Graefe's Archive for Clinical and Experimental Ophthalmology* **244**:199–204 DOI [10.1007/s00417-005-0006-7](https://doi.org/10.1007/s00417-005-0006-7).
- Lee BJ, Jun HO, Kim JH, Kim JH. 2019.** Astrocytic cystine/glutamate antiporter is a key regulator of erythropoietin expression in the ischemic retina. *FASEB Journal* **33**:6045–6054 DOI [10.1096/fj.201802144R](https://doi.org/10.1096/fj.201802144R).
- Lee D, Kang H, Yoon KY, Chang YY, Song HB. 2020a.** A mouse model of retinal hypoperfusion injury induced by unilateral common carotid artery occlusion. *Experimental Eye Research* **201**:108275 DOI [10.1016/j.exer.2020.108275](https://doi.org/10.1016/j.exer.2020.108275).
- Lee D, Miwa Y, Jeong H, Ikeda S-i, Katada Y, Tsubota K, Kurihara T. 2020b.** A murine model of ischemic retinal injury induced by transient bilateral common carotid artery occlusion. *JoVE* **1**:e61865 DOI [10.3791/61865](https://doi.org/10.3791/61865).
- Lee D, Tomita Y, Miwa Y, Jeong H, Mori K, Tsubota K, Kurihara T. 2021.** Fenofibrate protects against retinal dysfunction in a murine model of common carotid artery occlusion-induced ocular ischemia. *Pharmaceuticals* **14**(3):223 DOI [10.3390/ph14030223](https://doi.org/10.3390/ph14030223).
- Li Q, Zemel E, Miller B, Perlman I. 2002.** Early retinal damage in experimental diabetes: electroretinographical and morphological observations. *Experimental Eye Research* **74**:615–625 DOI [10.1006/exer.2002.1170](https://doi.org/10.1006/exer.2002.1170).
- Luo J, He T, Yang J, Yang N, Li Z, Xing Y. 2020.** SIRT1 is required for the neuroprotection of resveratrol on retinal ganglion cells after retinal ischemia-reperfusion injury in mice. *Graefe's Archive for Clinical and Experimental Ophthalmology* **258**:335–344 DOI [10.1007/s00417-019-04580-z](https://doi.org/10.1007/s00417-019-04580-z).
- Matei N, Leahy S, Auvazian S, Thomas B, Blair NP, Shahidi M. 2020.** Relation of retinal oxygen measures to electrophysiology and survival indicators after permanent. *Translational Stroke Research* **11**:1273–1286 DOI [10.1007/s12975-020-00799-9](https://doi.org/10.1007/s12975-020-00799-9).
- Miller RF, Dowling JE. 1970.** Intracellular responses of the Müller (glial) cells of mudpuppy retina: their relation to b-wave of the electroretinogram. *Journal of Neurophysiology* **33**:323–341 DOI [10.1152/jn.1970.33.3.323](https://doi.org/10.1152/jn.1970.33.3.323).

- Minhas G, Morishita R, Anand A. 2012.** Preclinical models to investigate retinal ischemia: advances and drawbacks. *Frontiers in Neurology* 3:75 DOI 10.3389/fneur.2012.00075.
- Miwa Y, Hoshino Y, Shoda C, Jiang X, Tsubota K, Kurihara T. 2019a.** Pharmacological HIF inhibition prevents retinal neovascularization with improved visual function in a murine oxygen-induced retinopathy model. *Neurochemistry International* 128:21–31 DOI 10.1016/j.neuint.2019.03.008.
- Miwa Y, Tsubota K, Kurihara T. 2019b.** Effect of midazolam, medetomidine, and butorphanol tartrate combination anesthetic on electroretinograms of mice. *Molecular Vision* 25:645–653.
- Ogishima H, Nakamura S, Nakanishi T, Imai S, Kakino M, Ishizuka F, Tsuruma K, Shimazawa M, Hara H. 2011.** Ligation of the pterygopalatine and external carotid arteries induces ischemic damage in the murine retina. *Investigative Ophthalmology & Visual Science* 52:9710–9720 DOI 10.1167/iovs.11-8160.
- Osborne NN, Casson RJ, Wood JPM, Chidlow G, Graham M, Melena J. 2004.** Retinal ischemia: mechanisms of damage and potential therapeutic strategies. *Progress in Retinal and Eye Research* 23:91–147 DOI 10.1016/j.preteyeres.2003.12.001.
- Qin Y, Ji M, Deng T, Luo D, Zi Y, Pan L, Wang Z, Jin M. 2019.** Functional and morphologic study of retinal hypoperfusion injury induced by bilateral common carotid artery occlusion in rats. *Scientific Reports* 9:80 DOI 10.1038/s41598-018-36400-5.
- Robson JG, Saszik SM, Ahmed J, Frishman LJ. 2003.** Rod and cone contributions to the a-wave of the electroretinogram of the macaque. *The Journal of Physiology* 547:509–530 DOI 10.1113/jphysiol.2002.030304.
- Shirao Y, Kawasaki K. 1998.** Electrical responses from diabetic retina. *Progress in Retinal and Eye Research* 17:59–76 DOI 10.1016/s1350-9462(97)00005-0.
- Sim DA, Keane PA, Zarranz-Ventura J, Fung S, Powner MB, Platteau E, Bunce CV, Fruttiger M, Patel PJ, Tufail A, Egan CA. 2013.** The effects of macular ischemia on visual acuity in diabetic retinopathy. *Investigative Ophthalmology & Visual Science* 54:2353–2360 DOI 10.1167/iovs.12-11103.
- Song Y, Gong Y, Xie Z-g, Li C-h, Gu Q, Wu XJAPS. 2008.** Edaravone (MCI-186), a free radical scavenger, attenuates retinal ischemia/reperfusion injury in rats. *Acta Pharmaceutica Sinica* 29:823–828 DOI 10.1111/j.1745-7254.2008.00822.x.
- Sun W, Geng Y, Chen YT, Tang XH, Zhang YJ, Gu SH, Xie JJ, Zhang ZA, T XS. 2019.** Differences of brain pathological changes and cognitive function after bilateral common carotid artery occlusion between Sprague-Dawley and Wistar rats. *Acta Physiologica Sinica* 71:705–716.
- Terelak-Borys B, Skonieczna K, Grabska-Liberek I. 2012.** Ocular ischemic syndrome - a systematic review. *Medical Science Monitor: International Medical Journal of Experimental and Clinical Research* 18:RA138–RA144 DOI 10.12659/msm.883260.
- Tomita Y, Lee D, Miwa Y, Jiang X, Ohta M, Tsubota K, Kurihara T. 2020.** Pemaflibrate protects against retinal dysfunction in a murine model of diabetic retinopathy. *International Journal of Molecular Sciences* 21:6243 DOI 10.3390/ijms21176243.

- Tomita Y, Ozawa N, Miwa Y, Ishida A, Ohta M, Tsubota K, Kurihara T. 2019.** Pemafibrate prevents retinal pathological neovascularization by increasing FGF21 level in a murine oxygen-induced retinopathy model. *International Journal of Molecular Sciences* **20**:5878 DOI [10.3390/ijms20235878](https://doi.org/10.3390/ijms20235878).
- Van Dongen J, Slagboom PE, Draisma HHM, Martin NG, Boomsma DI. 2012.** The continuing value of twin studies in the omics era. *Nature Reviews Genetics* **13**:640–653 DOI [10.1038/nrg3243](https://doi.org/10.1038/nrg3243).
- Vecino E, Rodriguez FD, Ruzafa N, Pereiro X, Sharma SC. 2016.** Glia-neuron interactions in the mammalian retina. *Progress in Retinal and Eye Research* **51**:1–40 DOI [10.1016/j.preteyeres.2015.06.003](https://doi.org/10.1016/j.preteyeres.2015.06.003).
- Venkat P, Chopp M, Chen J. 2015.** Models and mechanisms of vascular dementia. *Experimental Neurology* **272**:97–108 DOI [10.1016/j.expneurol.2015.05.006](https://doi.org/10.1016/j.expneurol.2015.05.006).
- Wachtmeister L. 1998.** Oscillatory potentials in the retina: what do they reveal. *Progress in Retinal and Eye Research* **17**:485–521 DOI [10.1016/s1350-9462\(98\)00006-8](https://doi.org/10.1016/s1350-9462(98)00006-8).
- Wellons Iii JC, Sheng H, Laskowitz DT, Burkhard Mackensen G, Pearlstein RD, Warner DS. 2000.** A comparison of strain-related susceptibility in two murine recovery models of global cerebral ischemia. *Brain Research* **868**:14–21 DOI [10.1016/S0006-8993\(00\)02216-2](https://doi.org/10.1016/S0006-8993(00)02216-2).
- Yamamoto H, Schmidt-Kastner R, Hamasaki DI, Yamamoto H, Parel JM. 2006.** Complex neurodegeneration in retina following moderate ischemia induced by bilateral common carotid artery occlusion in Wistar rats. *Experimental Eye Research* **82**:767–779 DOI [10.1016/j.exer.2005.09.019](https://doi.org/10.1016/j.exer.2005.09.019).
- Yang G, Kitagawa K, Matsushita K, Mabuchi T, Yagita Y, Yanagihara T, Matsumoto M. 1997.** C57BL/6 strain is most susceptible to cerebral ischemia following bilateral common carotid occlusion among seven mouse strains: selective neuronal death in the murine transient forebrain ischemia. *Brain Research* **752**:209–218 DOI [10.1016/S0006-8993\(96\)01453-9](https://doi.org/10.1016/S0006-8993(96)01453-9).
- Yonemura D, Kawasaki K. 1979.** New approaches to ophthalmic electrodiagnosis by retinal oscillatory potential, drug-induced responses from retinal pigment epithelium and cone potential. *Documenta Ophthalmologica* **48**:163–222 DOI [10.1007/bf00207350](https://doi.org/10.1007/bf00207350).